

Determination of Photolysis Frequencies and Quantum Yields for Small Carbonyl Compounds using the EUPHORE Chamber

Klaus Wirtz

Centro de Estudios Ambientales del Mediterráneo

Parque Tecnológico, C.\ Charles R. Darwin 14, 46980 Paterna, Valencia, Spain

(to be presented on the Combined US/German Environmental Chamber Workshop
Riverside, 1999)

Abstract

Small aldehydes are formed during the photochemical oxidation of many VOC's, olefins and terpenes in urban as well as in rural areas. Photolysis and reaction with the OH radical are the most important initiation reactions for the removal of these compounds conducting to the formation of peroxy radicals and in the case of photolytic decomposition, either to stable molecules or free radicals.

The photolysis frequencies for various small aldehydes were measured in the EUPHORE Smog Chambers by photolysing the aldehydes with natural sunlight. The actinic flux during the experiment was measured with a spectroradiometer. The decay of aldehydes and formation of products were analysed by FTIR spectroscopy, gas chromatography and HPLC. The major products are explained in the case of acetaldehyde, propionaldehyde and i-butyraldehyde by a mechanism involving a primary dissociation step which leads to the formation of free radicals. The product analysis for photolysis experiments of butyraldehyde, pentanal, 2-Methylbutyraldehyde and 3-Methylbutyraldehyde indicates that for these molecules two primary photodissociation steps occur which gives either stable molecules or free radicals. Integrated quantum yields can be calculated from the ratio of the theoretical photolysis frequency using the measured radiation data and known absorption cross-sections by assuming a quantum yield of unity and the measured photolytic decay rate. The results obtained can be employed in numerical models which describe the tropospheric degradation of these compounds in order to assess the importance of the additional radical production on the atmospheric oxidation capacity and ozone formation potential of the precursors VOCs.

Experimental

The experiments were performed in the outdoor Smog Chamber in Valencia, Spain. The reactor consists of a half spherical FEP (fluorine ethene propene) foil which is highly transparent to the short wavelength sunlight in the UVB with a total volume of about 195 m³. A detailed description of the photoreactors is given in Becker, 1996. Small quantities of the corresponding aldehyde were introduced by an air stream into the reactor and photolysed during most experiments in the presence of an OH tracer. A tracer was used instead of an OH radical scavenger because the addition of high concentration of an organic compound like cyclohexane would saturate a huge part of the IR bands and influence the product analysis. SF₆ as inert inorganic compound was introduced to measure the dilution throughout the experiment by analysing the collected FTIR spectra.

Apparatus

A FTIR spectrometer, NICOLET Magna 550, was operated with a liquid nitrogen cooled MCT detector with a resolution of 1 cm⁻¹. The optical path length was 553.5 m and the spectra were recorded every 10 minutes by co-adding 550 interferograms.

Two different gas chromatographs were used to measure either the decay of the reactants or the formation of the products. The first chromatograph, a Fisons GC-8000 was equipped with a 30 m DB-624 fused silica capillary column (J&W Scientific, 0.32 mm id, 1.8 μm film) and operated in a constant pressure mode. Two detectors were used in series, FID and PID (GC-PID), to obtain the chromatographic signals. The second chromatograph, a Fisons Trace-Gas-Analyser (TGA), which incorporates a cryogenic enrichment trap, was connected to a FID detector. 200 cm³ air were collected in a sampling loop at 120 °C and passed to a micro trap with Tenax cooled to -120°C with liquid N₂. The injection onto the chromatographic column (30 m DB-1, J&W Scientific, 0.25 mm id, 1.0 μm film) in splitless mode is achieved by a rapid heating of the micro trap to 240 °C.

The hydroperoxide analysis was based on the reaction of H₂O₂ and organic peroxides with *p*-hydroxyphenylacetic acid (POPHA) to produce a fluorescent dimer (6,6'-dihydroxy-3,3'-biphenyldiacetic acid) using peroxidase as an enzyme catalyst

(Gäb et al., 1995). The sampled hydroperoxides were separated on a Superspher 60 RP-Select B column using an Hewlett-Packard 1050 Series isocratic pump at a flow rate of 0.5 mL/min with H₃PO₄ buffer as mobile phase adjusted to pH=3.5 containing 4.9x10⁻⁸ mol/L of H₂O₂ to condition the column. The fluorescence of the biphenylic derivative was measured at an excitation wavelength of 285 nm and an emission wavelength of 410 nm. Detector response was proportional to the individual hydroperoxide concentration; quantification of the chromatographic signals was made injecting liquid H₂O₂ standards prepared from serial dilutions of H₂O₂ stock standards (Fluka, Sigma-Aldrich) assuming a similar response for the alkyl hydroperoxides. Air samples were collected with a flow rate of 2 L/min using the stripping technique (Lazrus et al., 1986; Lee et al., 1995). H₂O₂ and organic peroxides were stripped from the air into the collection solution using a continuous flow glass scrubbing coil. Collection solution (a H₃PO₄ buffer adjusted to pH=3.5) was pumped at 0.43 mL/min with a peristaltic pump (205S-BA Watson-Marlow). About 0.2 mL volume samples were taken in vials in periods varying from 5 to 15 min and analysed immediately by the HPLC-Fluorescence technique.

The light intensity was measured during the experiments with a calibrated spectroradiometer Bentham DM300. Special designed measurement heads with an uniform sensitivity with respect to the incident angle of the solar light are coupled through a quartz fibre bundle to the entrance optics of the monochromator. Two light beams, one for the direct light and the other for the reflected light, passed simultaneously but geometrical separated through the double monochromator. Independent detectors measure the light for both beams. The spectra were recorded every 5 min in the range from 290 nm to 520 nm with a spectral resolution of 1 nm FWHM.

Results and Discussion

Determination of Photolysis Frequencies and Effective Quantum Yields

All experiments were conducted at least for several hours at midday using the highest sun light intensity in the absence of nitrogen oxides, NO_x. In order to evaluate the photolysis frequency the loss rates obtained from the decay of the individual aldehydes (PID-GC data) were corrected for the dilution. There was no evidence found

from the decay rates of the tracer compounds that OH radical reactions may influence the calculated photolysis frequencies. The measured decay rates of the tracers overlap within the error limits with the dilution rate of the chamber. Different tracers were tested and selected to have a high OH rate constant whereby other loss processes like wall deposition or ozone reaction should be negligible. Isoprene as tracer has the highest OH rate constant and could be measured with high accuracy by GC as well as by FTIR, but the decay was influenced by the formed ozone. Cyclohexane showed the same properties with respect to the GC detection but due to the lower OH rate constant only high OH radical levels $>10^5$ /cm³ could be detected. Most experiments were performed using di-n-butyl ether as tracer which does not show a significant wall deposition and does not react with O₃. The detectable OH radical level with this tracer is in the range of 5×10^4 /cm³.

Table 1: Photolysis frequencies and calculated effective quantum yields.

Compound	Photolysis Frequency s ⁻¹	Photolysis Frequency J(NO ₂) s ⁻¹	Theoretical Loss Rate Q-yield 1 s ⁻¹	Effective Quantum yield	Literature Data on Quantum yields
Acetaldehyde	2.9×10^{-6}	10.7×10^{-3}	4.92×10^{-5}	0.06	0.4 300nm ^{&} 0.1 320nm
Propionaldehyde	1.1×10^{-5}	9.12×10^{-3}	3.57×10^{-5}	0.31	
Butyraldehyde	1.1×10^{-5}	9.92×10^{-3}	5.18×10^{-5}	0.21	
Isobutyraldehyde	3.3×10^{-5}	8.90×10^{-3}	4.67×10^{-5}	0.70	
Pentanal	1.6×10^{-5}	9.64×10^{-3}	5.52×10^{-5}	0.29	0.12 ^{&&}
2-Methyl butyraldehyde	3.8×10^{-5}	9.26×10^{-3}	$5.22 \times 10^{-5\#}$	0.72	
3-Methyl- butyraldehyde	1.3×10^{-5}	8.82×10^{-3}	$4.69 \times 10^{-5\#}$	0.27	
2-Pentanone	0.6×10^{-6}	7.03×10^{-3}	0.86×10^{-5}	0.07	

[#] Absorption cross section from Isobutyraldehyde used.

[&] Atkinson et al. (1989)

^{&&} Mean 300-320nm, T.J. Cronin and L. Zhu, 1998

The effective quantum yields were calculated as the ratio between the measured photolysis frequency and the theoretical photolysis frequency assuming a quantum yield of unity all over the absorption region of the individual carbonyl compound. The spectroradiometer data on the actinic flux was used to evaluate the theoretical value, which is the upper limit for the photo decomposition, according to the formula:

$$k \text{ (photolytic decay)} = \sum \mathbf{I}(\lambda) \sigma(\lambda) \phi(\lambda) \quad (\text{s}^{-1}),$$

with $\mathbf{I}(\lambda)$ the actinic flux, (measured by Bentham DM300) in photons $\text{cm}^{-2} \text{ s}^{-1}$ in the wavelength interval $\Delta\lambda$, centered at λ , absorption cross section $\sigma(\lambda)$ base e in $\text{cm}^2 \text{ molecule}^{-1}$ averaged over the wavelength interval $\Delta\lambda$ and centered at λ (Martinez et al. 1992) and quantum yield $\phi(\lambda)$, set to unity in the absorption region. The results obtained are given in Table 1.

Product Analysis

All experiments were performed in the absence of NO_x to avoid photo smog conditions where the decay of the aldehydes would be dominated by OH radical attack. Table 2 gives the main products observed by the different analytical techniques employed. As can be seen from Table 2 most of the products were identified by different methods and the product distribution is typical for NO_x -free conditions. A mechanism which explains the formed products in the case of butyraldehyde is given in Figure 1.

FIGURE 1: Postulated mechanism for the photolysis of butyraldehyde

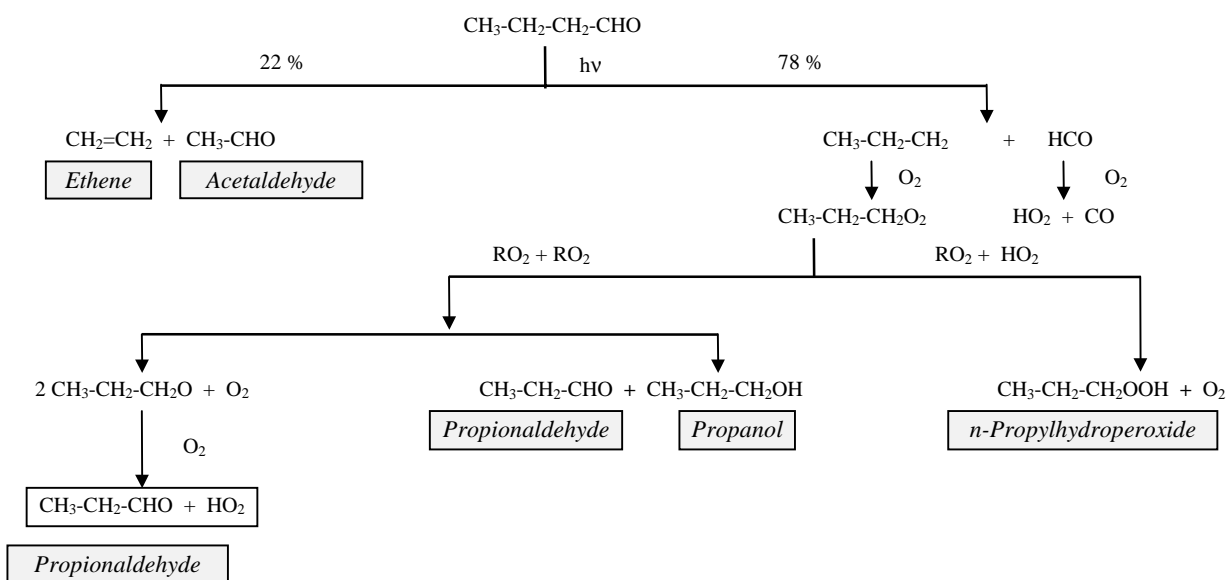


Table 2: Identified products during the photolysis experiments of the carbonyls

Carbonyl Compound	Products	Detection Method
Acetaldehyde CH₃CHO	Formaldehyde CO H ₂ O ₂ Methylhydroperoxide	FTIR FTIR HPLC-Fluorescence HPLC-Fluorescence
Propionaldehyde CH₃CH₂CHO	Formaldehyde CO Acetaldehyde Ethylhydroperoxide H ₂ O ₂	FTIR FTIR FTIR, GC-PID HPLC-Fluorescence, FTIR HPLC-Fluorescence
Butyraldehyde CH₃CH₂CH₂CHO	Formaldehyde CO Acetaldehyde Propionaldehyde 1-Propanol Ethene n-Propylhydroperoxide H ₂ O ₂	FTIR FTIR GC-PID GC-PID GC-TGA GC-PID, GC-TGA HPLC-Fluorescence HPLC-Fluorescence
Isobutyraldehyde CH₃CH(CH₃)CHO	CO Acetaldehyde Acetone Isopropanol Isopropylhydroperoxide H ₂ O ₂	FTIR, CO-Monitor GC-PID, FTIR GC-PID GC-TGA HPLC-Fluorescence HPLC-Fluorescence
Pentanal CH₃CH₂CH₂CH₂CHO	Acetaldehyde Butyraldehyde Propene n-Butylhydroperoxide (minor) CO (?)	GC-PID GC-PID GC-TGA, CG-PID HPLC-Fluorescence CO-Monitor
2-Methylbutyraldehyde CH₃CH₂CH(CH₃)CHO	Acetaldehyde CO 2-Butylhydroperoxide Ethene	GC-PID CO-Monitor HPLC-Fluorescence GC-TGA
3-Methylbutyraldehyde CH₃CH(CH₃)CH₂CHO	Propene Acetaldehyde Isobutyraldehyde Acetone CO i-Butylhydroperoxide	GC-PID GC-PID GC-PID, GC-TGA GC-TGA CO-Monitor HPLC-Fluorescence
2-Pentanone CH₃C(O)CH₂CH₂CH₃	Ethene Propionaldehyde Propylhydroperoxide Methylhydroperoxide	GC-TGA GC-TGA HPLC-Fluorescence HPLC-Fluorescence

In bold are the major products, underlined are products arising from a molecular channel.

For acetaldehyde, propionaldehyde and i-butyraldehyde all products could be observed which can be expected from the peroxyradical cross reactions $RO_2 + RO_2$ and $RO_2 + HO_2$ after dissociation into free radicals $R + HCO$. The photo decomposition of butyraldehyde, pentanal, 2-Methylbutyraldehyde and 3-Methylbutyraldehyde yields stable molecules and free radicals. The maximum alkylhydroperoxide concentrations measured at the end of the experiment are summarised in Table 3.

Table 3: Maximum values measured at the end of the photolysis experiments

Carbonyl Compound	H₂O₂ ppb	MHP ppb	EHP ppb	PHP ppb	i-PHP ppb	i-BHP ppb	1-BHP ppb	2-BHP ppb
Acetaldehyde	4.7	18.62						
Propionaldehyde	12.2	1.5	153.6					
Butyraldehyde	4.5	0.4	1.9	47.5				
i-Butyraldehyde	10.0				700			
Pentanal	1.2						3.5	
2-Methyl-butyr-aldehyde	5.7	4.9	36.1					243.7
3-Methyl-butyr-aldehyde	3.5					14.23		
2-Pentanone	2.5	4.6	0.4	7.0				

Carbonyls which decompose into stable molecules and free radicals are marked

A numerical simulation was performed using the Facsimile code given in the MCM-Master-Mechanism (M.Pilling, University of Leeds) in order to obtain the branching ratio for the primary photo dissociation step for butyraldehyde. According to the simulation results branching ratios of 0.78 for the free radical channel and 0.22 for of the photo decomposition into stable molecules, ethene and acetaldehyde, can be calculated. The comparison between the experimental data and the simulation is shown in Figure 2. Using this branching ratio and the effective quantum yield measured for n-butyraldehyde a quantum yield of 0.16 for the free radical channel and 0.05 for the molecular channel can be determined.

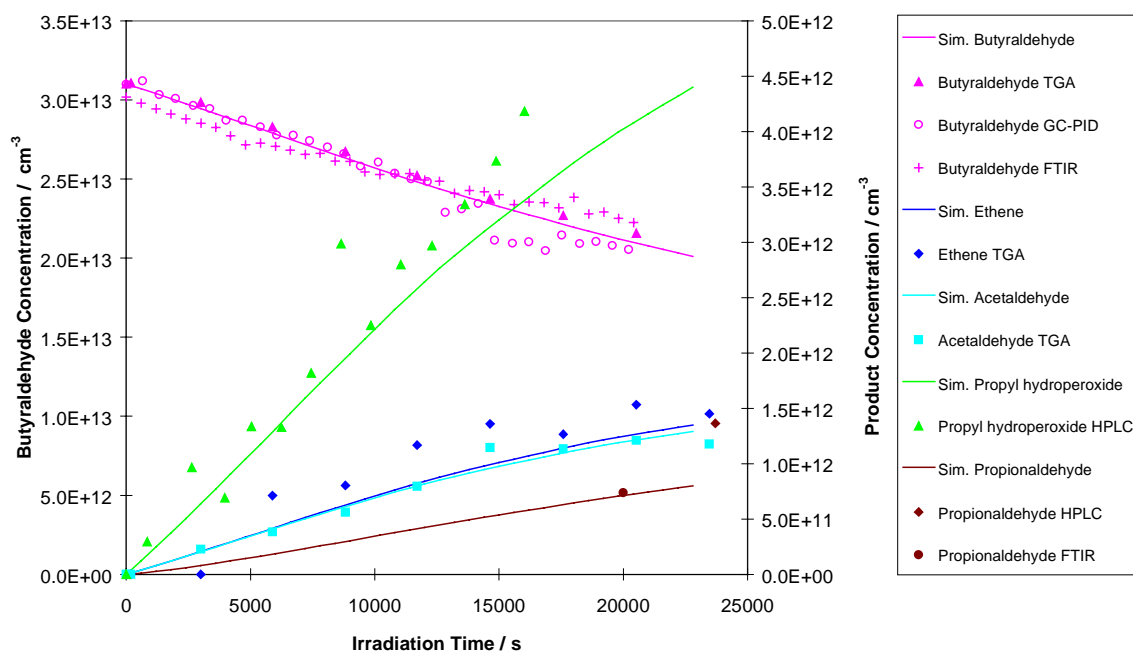


FIGURE 2: Simulation results from the butyraldehyde photolysis.

Conclusions

- ❑ Aldehydes with a chain length $< C_4$ decompose only into free radicals.
- ❑ For aldehydes with a chain length $\geq C_4$ the photo decomposition proceeds via two channels, a molecular channel and a free radical channel. The individual contribution for each channel depends on the molecular structure.
- ❑ The very low n-butyl hydroperoxide and CO concentrations measured in the case of n-pentanal indicate that the free radical channel is of minor importance for longer chain aldehydes.
- ❑ The effective quantum yields for all compounds investigated is below unity. The highest values were obtained for aldehydes which has a structure like $R-CH(CH_3)CHO$
- ❑ Alkyl hydroperoxide formation can be used to track free radicals formed from the photo decomposition of carbonyls to determine the individual decomposition pathways. The method will be employed to measure the effective quantum yields for ketones.
- ❑ The effective quantum yields for longer chain ketones like 2-pentanone is quite below unity and similar as determined for acetone (Gardner et al., 1984).

References

- Atkinson R., D.L. Baulch, R.A. Cox, R.F. Hampson, Jr., A.J. Kerr and J. Troe, *J. Phys. Chem. Ref. Data* **18** (1989), 881-1097.
- Becker, K.H. (ed); *The European Photoreactor EUPHORE*. Final Report of the EC-Project EV5V-CT92-0059, Wuppertal, Germany (1996).
- Cronin, T.J. and L. Zhu, *J. Phys. Chem.* **102** (1998), 10274-10279.
- Lazrus A.L., G.L.Kok, J.A. Lind, S.N. Gitlin, B.G. Heikes and R.E. Shetter; *Anal. Chem.* **58** (1986) 594-597.
- Lee M., B.C. Noone, D. O'Sullivan B.G. and Heikes; *J. Atmos. Ocean. Tech.* **12** (1995) 1060-1070.
- Gäb S., W.V. Turner, S. Wolff, K.H. Becker, L. Ruppert and K.J. Brockmann; *Atmos. Environ.* **29** (1995) 2401-2407.
- Possanzini M., V. Di Palo, M. Petricca, R. Fratarcangelli and D. Brocco; *Atmos. Environ.* **30** (1996) 3757-3764.
- Shepson P.B., Hastie D.R., Schiff H.I., M. Polizzi, J.W. Bottenheim, K. Anlauf, G.I. Mackay and D.R. Karecki; *Atmos. Environ.* **25A** (1991) 2001-2015.

Acknowledgements This work has been supported by the European Commission through the project ENV4-CT97-0419. The authors want to thank the financial contribution of the Generalitat Valenciana and Fundación BANCAJA.